Optics Letters

Observation of stable-vector vortex solitons

Yana Izdebskaya,[1,*] Gaetano Assanto,[2,3] and Wieslaw Krolikowski[1,4]

[1]Laser Physics Center, Research School of Physics and Engineering, The Australian National University, Canberra ACT 0200, Australia
[2]NooEL–Nonlinear Optics and OptoElectronics Lab, Department of Electronic Engineering, University of Rome "Roma Tre," 00146 Rome, Italy
[3]Optics Laboratory, Tampere University of Technology, FI-33101 Tampere, Finland
[4]Texas A&M University at Qatar, Doha, Qatar
*Corresponding author: yvi124@rsphysse.anu.edu.au

Received 27 July 2015; accepted 11 August 2015; posted 17 August 2015 (Doc. ID 246496); published 1 September 2015

We report on the first experimental observation of stable-vector vortex solitons in nonlocal nonlinear media with a reorientational response, such as nematic liquid crystals. These solitons consist of two co-polarized, mutually trapped beams of different colors, a bright fundamental spatial soliton, and a nonlinear optical vortex. The nonlinear vortex component, which is normally unstable in nonlinear media, is stabilized and confined here by the highly nonlocal refractive potential induced by the soliton.

OCIS codes: (190.6135) Spatial solitons; (190.5940) Self-action effects; (050.4865) Optical vortices; (160.3710) Liquid crystals.

http://dx.doi.org/10.1364/OL.40.004182

Optical vortices are intriguing objects that have attracted quite a bit of attention [1–3] because of their fascinating properties and potential applications in the optical encoding/processing of information [4–7], as well as in tweezers and guiding and trapping particles [8–11]. Vortex beams have a toroid-shaped intensity profile with a characteristic screw-type phase dislocation at the zero-intensity point where the electromagnetic field vanishes. Such complex beams can be generated and propagate in either linear or nonlinear media, but in the presence of a self-focusing response they become highly unstable due to a symmetry-breaking azimuthal instability, and decay into several fundamental solitons [12,13]. Thus, vortex localization in a nondiffracting, nonlinear mode (a vortex soliton) and its stabilization against azimuthal instabilities are among the current challenges in the nonlinear optics of complex wavepackets.

Early numerical studies revealed that spatially localized vortices can be stabilized in highly nonlocal, nonlinear media with a self-focusing response [14,15], as later confirmed by experimental results on the existence of stable, single-charge vortex solitons in thermo-optical nonlocal media [16]. Nonlocal spatial solitons were also found to be able to guide and route vortex beams across an interface or around a defect, acting against diffraction and instabilities enhanced by a perturbation [17]. In the nonlinear regime, an intense vortex and a spatial soliton in a nonlocal medium are expected to form vector solitons [12], similar to the cases of vector solitons with bright beam components of different colors in nonlocal media [18,19], spiraling solitons with angular momentum [20–22], and multi-hump soliton structures consisting of two (or more) components that mutually self-trap [12,23,24]. As shown in recent theoretical/numerical studies [25], such two-component vector vortex solitons are expected to exist as stable states in nematic liquid crystals (NLCs), owing to the highly nonlocal response of the medium [26,27] and the stabilizing character of the resulting nonlinear, nonlocal potential generated by the superposition of both beam components [25,28]. However, in spite of the numerous theoretical studies of vector vortex solitons, such localized beams have not been observed in experiments so far. On the contrary, to date, such multi-component spatial vortex solitons were found to undergo strong instabilities and eventually break up [13,29].

In this Letter, for the first time to the best of our knowledge, we experimentally demonstrate the formation of two-component, two-color vector solitons in which one of the components is an optical vortex and the other a bright spatial soliton. Employing nematic liquid crystals as the nonlinear medium, we show how the nonlocal, nonlinear reorientational response can dramatically enhance the mutual field coupling through the light-induced potential, leading to the stabilization of the nonlinear vortex beam when the power of the solitary beam exceeds a certain value.

NLCs are molecular liquids with a large degree of orientational (angular) order and no positional order. Most NLCs are positive uniaxials with a large optical birefringence $\Delta\varepsilon$ from 0.1 to 0.7 in the optical spectrum, with a refractive index that is higher for a beam polarized along the optic axis (or director) $\hat{\mathbf{n}}$. Typical NLCs are also spatially nonlocal due to the elastic links between the molecules and, most importantly, they are excellent all-optical materials by virtue of their reorientational response to electric fields. An intense electric field $\mathbf{E}$ oriented at a finite angle (nonzero and $\neq \pi/2$) with the director $\hat{\mathbf{n}}$ induces a dipole moment in the molecules, which then can rotate in order to minimize the overall system energy (electromagnetic and elastic). The torque is orthogonal to the principal plane of an extraordinary wave and has the form

$$\Gamma = \Delta\epsilon(\hat{\mathbf{n}}\cdot\mathbf{E})(\hat{\mathbf{n}}\wedge\mathbf{E}). \quad (1)$$

When the equilibrium between the torque and the elastic forces present through the intermolecular links and anchoring is

reached, light propagation is ruled by molecular reorientation. In a standard NLC, the latter increases the angle ψ between the optic axis and the wave vector, thereby increasing the refractive index for an extraordinarily polarized field. This yields self-focusing and, eventually, the spatial localization of a bright beam in the form of a spatial soliton, i.e., a *nematicon* [27].

In our experiments, we used a planar cell formed by two poycarbonate slides held parallel at a distance of 110 μm across y, containing the NLC mixture 6CHBT. The maximum propagation length along the z axis was 1.1 mm from the input to the output facets. The latter were defined and sealed by two additional 150 μm -thick slides attached perpendicularly to z in order to prevent the formation of exposed menisci. The mean angular orientation of the NLC optic axis was preset by mechanically rubbing the internal interfaces at an angle $\psi_0 = \pi/4$ with respect to z in the plane (x, z), parallel to the slides.

Figure 1 shows a sketch of the experimental setup for the generation of two-component, two-color vector vortex solitons. One component (red) carries the single-charge vortex beam generated with a fork-type amplitude diffraction hologram (DH) using extraordinarily polarized light from a cw laser beam at wavelength $\lambda_1 = 671$ nm and power P_r. The vortex beam is launched into the NLC cell with a 10× microscope objective (MO_1), resulting in an input ring with a radius of $w \approx 7$ μm (defined by its peak intensity). The second (green) component is an extraordinarily polarized fundamental Gaussian beam of wavelength $\lambda_2 = 532$ nm and power P_g. The co-polarized, two-color components are co-launched with parallel wave vectors along z into the NLC. The transverse dynamics of each beam in the medium were monitored by collecting the light transmitted through the output interface, using a 20× microscope objective (MO_2) and a high-resolution CCD camera. To separately record the output images of the (red) vortex or green (fundamental) beams, we used either red or green filters placed in front of the camera.

First, we studied the behavior of each component propagating independently in the cell with various input powers. Figure 2 shows the input [Figs. 2(a) and 2(b)] and output [Figs. 2(c)–2(f)] profiles of each beam: the green Gaussian (left) and the red charge-1 vortex (right). At low input powers, when

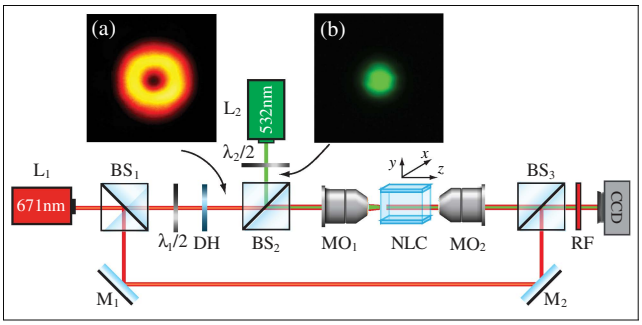

Fig. 1. Experimental setup: $L_{1,2}$ are the green ($\lambda_1 = 671$ nm) and red ($\lambda_2 = 532$ nm) cw lasers. $\lambda/2$: half-wave plates; BS: beam splitters; DH: vortex hologram; M: mirrors; MO_1:10 × microscope objective; MO_2:20 × microscope objective; NLC: sample; RF: red bandpass filter; CCD: charge-coupled device camera. Insets (a) and (b) show the transverse intensity distributions of the input vortex and Gaussian beams, respectively.

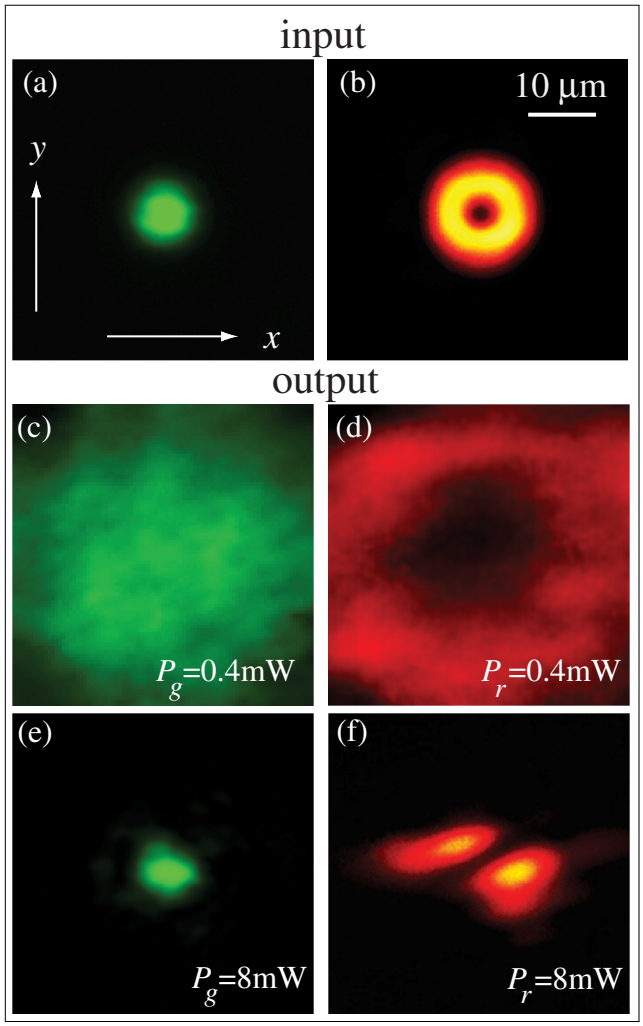

Fig. 2. Experimental results depicting the behavior of each vector beam component, i.e., a Gaussian (left, green) or a single-charge vortex (right, red) propagating separately in the NLC cell. (a), (b) Input profiles of each component. (c)–(f) Output profiles of beam components for various levels of input powers P_g and P_r for the Gaussian (green) and the vortex (red) components, respectively.

$P_{g,r} < 0.9$ mW, both beams diffract without any appreciable nonlinear self-action [see Figs. 2(c) and 2(d)]. As P_g increases, the green beam undergoes self-focusing and the transverse intensity distribution at the output visibly shrinks, giving rise to a nematicon for $P_g > 2.4$ mW [see Fig. 2(e)]. By increasing the power in the component that carries angular momentum to $P_r > 5$ mW, the vortex beam also experiences self-focusing, but its initially radial symmetry distribution breaks up into a pair of filaments [Fig. 2(f)] as a result of the azimuthal instability enhanced by the nonsymmetrical configuration of the planar cell and the related anisotropy in the induced refractive index profile. Such dynamics are perfectly consistent with the results reported earlier, when we experimentally observed the astigmatic transformations of vortex beams into spiraling dipole azimuthons [13].

In order to stabilize the vortex beam and prevent its breakup, we investigated the incoherent, nonlinear interaction of two color (green and red) components (a vortex and a

Gaussian) propagating simultaneously in the cell as vector beam. Both beams were extraordinarily polarized, i.e., with their input electric field directed along y. In these experiments, we changed the input power of the green beam P_g, while the power of the input red vortex beam P_r was kept constant at 8 mW, which is high enough to excite nonlinear effects and instabilities in the absence of the fundamental soliton. For $P_g < 2.4$ mW, the vortex exhibited clear azimuthal instability and transformed into a dipole-like transverse intensity distribution [compare Figs. 2(f) and 3(a)]. In this regime, the beam behaved similar to the dipole-like vector soliton observed in other systems [30,31]. At higher power, where $P_g > 2.6$ mW, we clearly observed a profile reshaping of the red component of this dipole-mode vector soliton [see Fig. 3(b)]. A further increase in the power $4.9 < P_g$ [mW]<8 led to a remarkable profile transformation: the dipole-like beam transformed into a perfect ring structure, forming a stable-vector vortex soliton with its annular shape around a dark core [see Fig. 3(c)]. At higher excitations, (not shown) the spatial dynamics were amplified as the beam developed irregular and temporally unstable structures [32].

Finally, in order to confirm the presence of a phase singularity in the vector vortex soliton, we investigated its phase structure by arranging a Mach–Zehnder interferometer in our experimental setup (beam splitters BS_1 and BS_3 and mirrors M_1 and M_2 in Fig. 1). A slightly tilted, relatively wide, red Gaussian beam was made to interfere with the vortex component at the output. The interferogram in Fig. 3(d) allowed for the detection of phase dislocations by the characteristic presence of fork dislocations. Therefore, we ascertained that the vortex character of the red input beam was retained after the formation of the vector soliton, owing to the interaction with the nonlocal potential induced in the medium by the green nematicon. The highly nonlocal, nonlinear response of the soft matter, specifically, reorientational nematic liquid crystals, dramatically enhanced the incoherent field coupling of the two co-polarized wave-packets of different colors, leading to the stabilization of the vortex soliton when the soliton power was large enough to trap the nonlinear vortex.

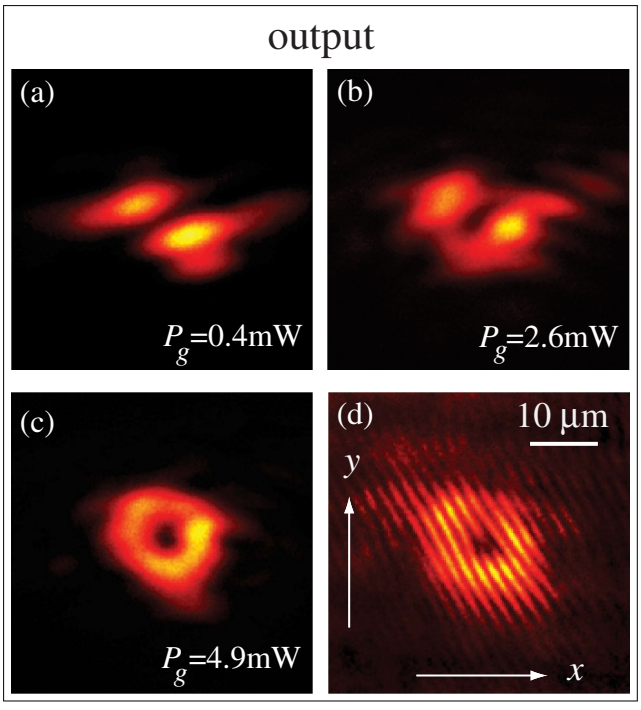

Fig. 3. Experimentally observed output intensity distribution of the vortex component of the composite beam in the NLC cell for various input powers of the fundamental (Gaussian) component P_g. (a), (b) Azimuthal instability of the vortex and its breakup into a dipole-like structure for low powers of the fundamental (Gaussian) component. (c) Stable propagation of the vortex beam as the component of the stable vector nematicon. (d) Corresponding interferogram confirming its vortex nature.

In conclusion, we have experimentally demonstrated the existence of stable, two-component, two-color vector vortex solitons in nematic liquid crystals. These vector solitons appear in the form of two-wavelength self-trapped beams, with one of the components carrying a phase singularity and being stabilized by the nonlocally enhanced interaction with the other localized beam, a fundamental spatial soliton. We found that these vector beams can be generated using nematicons with input powers within a certain range of excitation. We expect that such a first report on nonlinear vortex stabilization and trapping by coaxial spatial solitons will stimulate further research on vortex routing in various systems, including nonlocal nonlinearities [17,33] and nematic liquid crystals [34,35].

Funding. Academy of Finland (282858); Australian Research Council.

Acknowledgment. Y. Izdebskaya would like to thank Yu. Kivshar for useful discussions.

REFERENCES

1. J. F. Nye and M. V. Berry, Proc. R. Soc. London A **336**, 165 (1974).
2. A. M. Yao and M. J. Padgett, Adv. Opt. Photon. **3**, 161 (2011).
3. G. A. Swartzlander, *Optical Vortices* (CRC Press, 2014).
4. E. Brasselet and C. Loussert, Opt. Lett. **36**, 719 (2011).
5. E. Brasselet, Phys. Rev. Lett. **108**, 087801 (2012).
6. R. Barboza, U. Bortolozzo, G. Assanto, E. Vidal-Henriquez, M. G. Clerc, and S. Residori, Phys. Rev. Lett. **111**, 093902 (2013).
7. J. Wang, J.-Y. Yang, I. M. Fazal, N. Ahmed, Y. Yan, H. Huang, Y. Ren, Y. Yue, S. Dolinar, M. Tur, and A. E. Willner, Nat. Photonics **6**, 488 (2012).
8. D. G. Grier, Nature **424**, 810 (2003).
9. M. Padgett and R. Bowman, Nat. Photonics **5**, 343 (2011).
10. V. G. Shvedov, A. V. Rode, Y. V. Izdebskaya, A. S. Desyatnikov, W. Krolikowski, and Y. S. Kivshar, Phys. Rev. Lett. **105**, 118103 (2010).
11. V. G. Shvedov, A. S. Desyatnikov, A. V. Rode, Y. V. Izdebskaya, W. Z. Krolikowski, and Y. S. Kivshar, Appl. Phys. A **100**, 327 (2010).
12. Y. S. Kivshar and G. P. Agrawal, *Optical Solitons: From Fibers to Photonic Crystals* (Academic, 2003).
13. Y. V. Izdebskaya, A. S. Desyatnikov, G. Assanto, and Y. S. Kivshar, Opt. Express **19**, 21457 (2011).
14. A. I. Yakimenko, Y. A. Zaliznyak, and Y. S. Kivshar, Phys. Rev. E **71**, 065603 (2005).
15. D. Briedis, D. E. Petersen, D. Edmundson, W. Krolikowski, and O. Bang, Opt. Express **13**, 435 (2005).
16. C. Rotschild, O. Cohen, O. Manela, M. Segev, and T. Carmon, Phys. Rev. Lett. **95**, 213904 (2005).
17. G. Assanto, A. A. Minzoni, and N. F. Smyth, Opt. Lett. **39**, 509 (2014).
18. A. Alberucci, M. Peccianti, G. Assanto, A. Dyadyusha, and M. Kaczmarek, Phys. Rev. Lett. **97**, 153903 (2006).

19. B. D. Skuse and N. F. Smyth, Phys. Rev. A **79**, 063806 (2009).
20. A. Fratalocchi, A. Piccardi, M. Peccianti, and G. Assanto, Opt. Lett. **32**, 1447 (2007).
21. A. Fratalocchi, A. Piccardi, M. Peccianti, and G. Assanto, Phys. Rev. A **75**, 063835 (2007).
22. G. Assanto, N. F. Smyth, and A. L. Worthy, Phys. Rev. A **78**, 013832 (2008).
23. Z. Xu, Y. V. Kartashov, and L. Torner, Phys. Rev. E **73**, 055601 (2006).
24. Y. V. Kartashov, L. Torner, V. A. Vysloukh, and D. Mihalache, Opt. Lett. **31**, 1483 (2006).
25. Z. Xu, N. F. Smyth, A. A. Minzoni, and Y. S. Kivshar, Opt. Lett. **34**, 1414 (2009).
26. C. Conti, M. Peccianti, and G. Assanto, Phys. Rev. E **91**, 073901 (2003).
27. M. Peccianti and G. Assanto, Phys. Rep. **516**, 147 (2012).
28. A. A. Minzoni, N. F. Smyth, Z. Xu, and Y. S. Kivshar, Phys. Rev. A **79**, 063808 (2009).
29. Y. V. Izdebskaya, J. Rebling, A. S. Desyatnikov, and Y. S. Kivshar, Opt. Express **37**, 767 (2012).
30. W. Krolikowski, E. A. Ostrovskaya, C. Weilnau, M. Geisser, G. McCarthy, Y. S. Kivshar, C. Denz, and B. Luther-Davies, Phys. Rev. Lett. **85**, 1424 (2000).
31. Y. Zhang, Z. Wang, Z. Nie, C. Li, H. Chen, K. Lu, and M. Xiao, Phys. Rev. Lett. **106**, 093904 (2011).
32. Y. V. Izdebskaya, A. S. Desyatnikov, G. Assanto, and Y. S. Kivshar, Opt. Lett. **36**, 184 (2011).
33. G. Assanto and N. F. Smyth, J. Lasers Opt. Photon. **1**, 1000105 (2014).
34. G. Assanto, A. A. Minzoni, and N. F. Smyth, Phys. Rev. A **89**, 013827 (2014).
35. G. Assanto and N. F. Smyth, IEEE J. Sel. Top. Quantum Electron. (2015), in press.